

Cite this article as: Wang Jingze, Yin Jiaqing, Cui Jianwen, et al. Intergranular Reaction Mechanism of Submicron-Activated Mo-15Cu Alloy[J]. Rare Metal Materials and Engineering, 2023, 52(02): 448-453.

ARTICLE

Intergranular Reaction Mechanism of Submicron-Activated Mo-15Cu Alloy

Wang Jingze¹, Yin Jiaqing¹, Cui Jianwen², Chang Jing¹, Yu Yandong¹, Sun Yunlong¹

¹ School of Materials Science and Chemical Engineering, Harbin University of Science and Technology, Harbin 150040, China; ² College of Intelligent Systems Science and Engineering, Harbin Engineering University, Harbin 150006, China

Abstract: In order to investigate the intergranular reaction mechanism during sintering of molybdenum-copper powders with submicron components, a Mo-15Cu composite with an intergranular reaction layer was prepared by a submicron-activated layer method. The histomorphology, connectivity and structural characteristics of Mo-15Cu alloy were characterized by X-ray diffractometer (XRD), scanning electron microscope (SEM), energy dispersive spectrometer (EDS), transmission electron microscope (TEM), and high-resolution transmission electron microscope (HRTEM). The effect of submicron-activated layers on the intergranular reaction of Mo-15Cu composites was investigated. The results show that the submicron-activated layer with a thickness of 0.5 μm is formed by adding 8wt% submicron powder. The submicron-sized Mo particles change the intergranular reaction mechanism through flow and diffusion, forming an intergranular reaction layer with a thickness of about 5 nm and achieving metallurgical bonding.

Key words: Mo-Cu pseudo-alloys; nano-twin; intergranular reaction layer; submicron-activated layer; metallurgical bonding

As a typical pseudo-alloy, Mo(W)-Cu alloy is widely used in electrical contacts, electronic packaging, heat dissipation materials and other fields^[1-3] due to its excellent properties such as thermal and electrical conductivity, resistance to arc ablation and good plasticity^[4-5]. Compared to W-Cu composites, Mo-Cu has low cost and lower density, stronger plastic forming ability and resistance to arc ablation^[6], and is widely studied and applied in the fields of high power integrated circuits, lightweighting, electronic packaging and electrical contacts^[7-8]. Pseudo-alloys composed of immiscible molybdenum-copper with significantly different melting points are attractive due to the combination of mechanical and physical properties of molybdenum and copper^[9]. Unfortunately, metallurgical bonding is one of the difficulties in the application of conventional molybdenum-copper pseudo-alloys, and plastic deformation can lead to disintegration at the interface, creating voids, cracks and other defects that can significantly weaken the mechanical and electrical properties.

The common methods of powder metallurgy for the preparation of molybdenum-copper alloys include mechanical activation and nanopowder sintering^[10-11], while mechanical

activation method cannot solve the problems of introduction of impurities and low efficiency. During the preparation process, the sinterability and densification of the powder are closely related to the powder properties, such as particle size and shape. Shon^[12] studied the effect of particles on powder packing density and flowability. Nanopowder sintering method can reduce the sintering temperature and increase the sample density, especially for nanoparticles^[13]. Nanomolybdenum powder can improve sintering activity, reduce sintering temperature, improve the density and properties of molybdenum-copper alloy, so that it can be used in high-performance electronic packaging, heat sinks, and high-power integrated circuits. A lot of studies on nanopowder sintered molybdenum-copper alloys have been reported, mainly focused on the preparation and property improvement of molybdenum-copper alloys^[14], while the nanopowder sintering method cannot avoid the problems such as high cost and low green density due to agglomeration. In this study, a Mo-15Cu alloy with an intergranular reaction layer was prepared by submicron-activation, and the intergranular reaction mechanism was investigated under the effect of submicron-

Received date: March 23, 2022

Foundation item: Project supported by the Reform and Development of Local Colleges and Universities of the Central Government of China (323210001); Project supported by the Harbin Talents of China (2015RAQXJ036)

Corresponding author: Cui Jianwen, Ph. D., College of Intelligent Systems Science and Engineering, Harbin Engineering University, Harbin 150006, P. R. China, E-mail: cjwben@163.com

Copyright © 2023, Northwest Institute for Nonferrous Metal Research. Published by Science Press. All rights reserved.

activation.

1 Experiment

Fig. 1 shows the schematic diagram of the submicron-activation layer construction. Micron molybdenum powder with a particle size of about 20 μm and nano molybdenum powder with a particle size of about 0.5 μm were used as raw powders. They were mixed to be Mo (micron)-Mo (submicron) powders with the mass ratio of 92:8. The submicron powder ratio was calculated by theoretical calculation of the model, the spiral mill was used for the mixing process, and the powder motion trajectory is shown in Fig. 2. The diameter of the threaded cutter was 10 mm, the diameter of the barrel was 20 mm, the speed was 2000 r/min, and the duration was 3 h. The mixed molybdenum powder was pressed in a steel mold of Φ25 mm×5 mm in size at room temperature under 120 MPa pressure and held for 10 s. The pressed billets were firstly heated to 300 °C with a holding time of 0.5 h. Secondly, the specimens were heated to 650 °C with a holding time of 2 h. Finally, the compacts were heated to 850 °C with a holding time of 3 h and the molybdenum skeleton was obtained by furnace cooling. The molybdenum skeleton was infiltrated by copper at 1100 °C for 2 h. X'PERT PRO MPD type X-ray diffractometer (XRD) was used for the analysis of

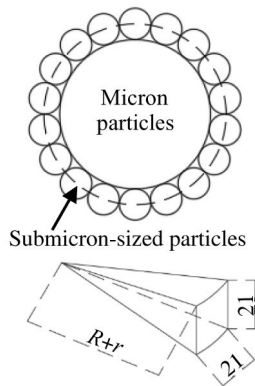


Fig.1 Schematic diagram of submicron-activated layer construction

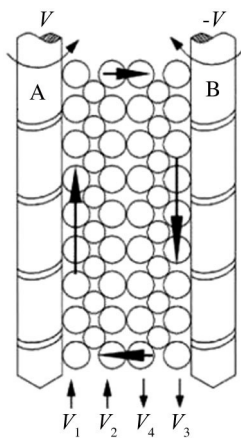


Fig.2 Schematic diagram of powder movement path

Mo skeleton and Mo-15Cu alloy; GX71-6230 optical microscope (OM) and SUS8020 scanning electron microscope (SEM) were used to observe the microstructure morphology; EDS was used to observe the distribution of molybdenum and copper elements by surface scanning and line scanning of the alloy; JEM-2100 transmission electron microscope (TEM) was used to observe the interface.

Fig. 3 shows the activation mechanism of the submicron powder. The submicron powder mass is determined by Eq.(1):

$$m = N_1 N_2 m_2 = \frac{180^2 M r^3}{\pi R^3 \theta^2} \tag{1}$$

where M is the micron particle mass, R is the micron particle radius, m is the nanoparticle mass, r is the nanoparticle radius, and θ is the angle of the circle center between two submicron-sized particles.

In order to verify the rationality of the above theory, the experimental verification analysis was performed, in which M was 18 g, R was 20 μm, and r was 0.5 μm. The mass of submicron powder was 1.486 g after theoretical calculation, accounting for 7.63% of the total mass. In view of the fact that the quadrilateral arrangement is not a dense arrangement, the mass of submicron powder was chosen to be 8% of the total mass.

2 Results and Discussion

2.1 Submicron-activated layer characterization

Fig.4 shows the microstructure of the molybdenum skeleton, in which the bright area is the molybdenum skeleton and the black area is the pores. The image shows that the

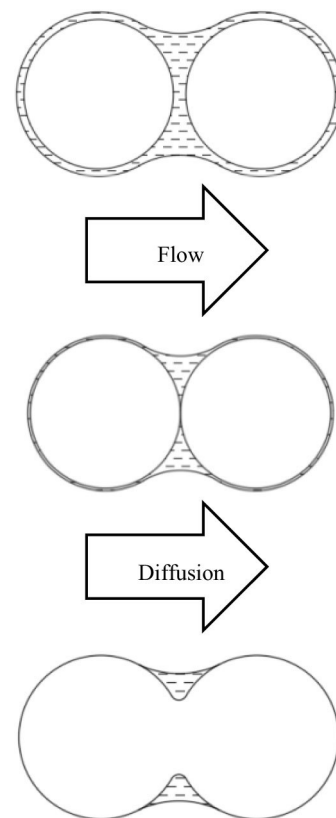


Fig.3 Diagram of submicron powder flow diffusion

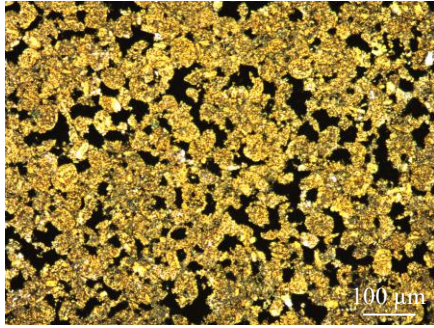


Fig.4 OM microstructure of Mo skeleton

molybdenum skeleton has few pores, continuous skeleton, regular shape and high density. The black stripes are composed of submicron powder particles with a small particle size, indicating that the submicron-sized particles are mainly distributed between micron particles. According to the relationship between particle surface energy and particle size^[15-16], preferential sintering occurs between submicron-sized particles, and submicron powder adheres to the surface of micron particles to form a submicron-activated layer, which reduces the continuity of micron particles and improves the continuity of the molybdenum skeleton.

Fig.5 shows SEM images of the molybdenum skeleton and Mo-15Cu alloy. Fig. 5a clearly shows the submicron-sized particles attached to micron particles to form a submicron-activated layer, and microparticles and submicron-sized particles form a microparticle-submicron-sized particle-microparticle mode that facilitates diffusion^[17]. In Fig.5b, phase I is the flow of molybdenum submicron powder, phase II is the atomic diffusion crystallization, and phase III is the sintered neck formation growth. The good mobility of submicron-sized

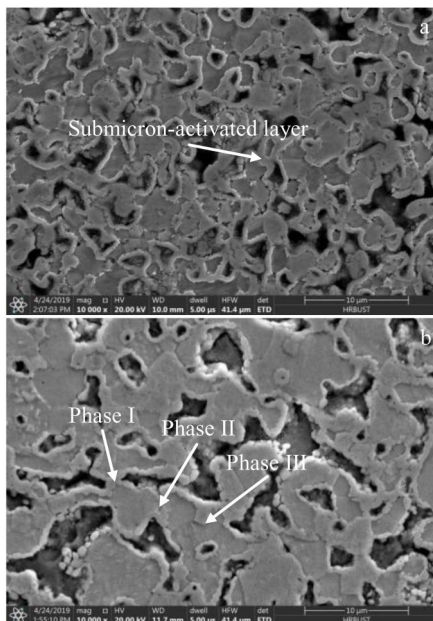


Fig.5 SEM images of molybdenum skeleton (a) and Mo-15Cu alloy (b)

particles based on van der Waals forces provides a more convenient diffusion condition and particle flow basis for the formation of sintering necks, and thus the integrity of the submicron-activated layer has a significant effect on the sintering density and strength.

The distribution of elements within the Mo-15Cu alloy is shown in Fig.6, in which the red particles are the molybdenum element and the green particles are the copper element. Fig.6b shows the EDS layering diagram, and Fig.6c and 6d show the elemental distribution. The distribution of molybdenum and copper elements is uniform, and copper element diffuses uniformly into the molybdenum skeleton. On the one hand, the addition of submicron-sized particles^[18] accelerates the atomic diffusion on the surface of the powder particles to facilitate the formation of sinter necks. On the other hand, it provides diffusion channels for the diffusion of copper elements, which promotes the occurrence of interfacial reactions, accelerates the generation of intergranular reaction layers, and enhances the connection of the molybdenum-copper interface.

To further determine the distribution of copper element in the alloy, EDS line scan analysis of the copper channels in the alloy is shown in Fig.7. The molybdenum content decreases and the copper content increases in the copper channels according to the elemental distribution of the linear scan. It indicates that the channels surrounded by the submicron-activated layers in the alloy have good connectivity during the copper infiltration process, which is beneficial to the copper infiltration. In the region of submicron-activated layer, the content of molybdenum tends to decrease and the content of copper tends to increase. The capillary forces between the submicron-sized particles facilitate the infiltration of liquid phase copper and the diffusion of copper elements into the molybdenum skeleton to form intergranular reaction layers.

2.2 Interfacial characterization of Mo-15Cu alloys

Fig.8 shows the TEM image of the Mo-15Cu alloy. The crystallographic features of the molybdenum and copper phases are obtained by diffraction analysis of selected areas^[19-20]. Fig.8b and 8c show the SAED pattern of Mo and Cu, respectively. The molybdenum phase grows into the copper phase, the copper phase wraps around the molybdenum phase. An obvious reaction layer is formed between the molybdenum phase and the copper phase with a width of 5 nm, which enhances the grain boundary strength. The reason why there are a large number of dislocations in the copper phase is the low hardness of copper phase.

Fig.9 shows the diffusion layers at the Mo/Mo and Mo/Cu interfaces. The local diffraction analysis of the diffusion layer between the molybdenum phases (Fig.9b) shows that planetary spots appear around the base point. Planetary spots are formed by secondary diffraction of a series of parallel overlapping lattice faces, which may form moire at the diffusion interfaces^[21]. During the sintering process, the high dislocation density releases stress and reduces the atomic mismatch, leading to the formation of satellite spots at the interfacial layer between the molybdenum phases. The Mo-Cu

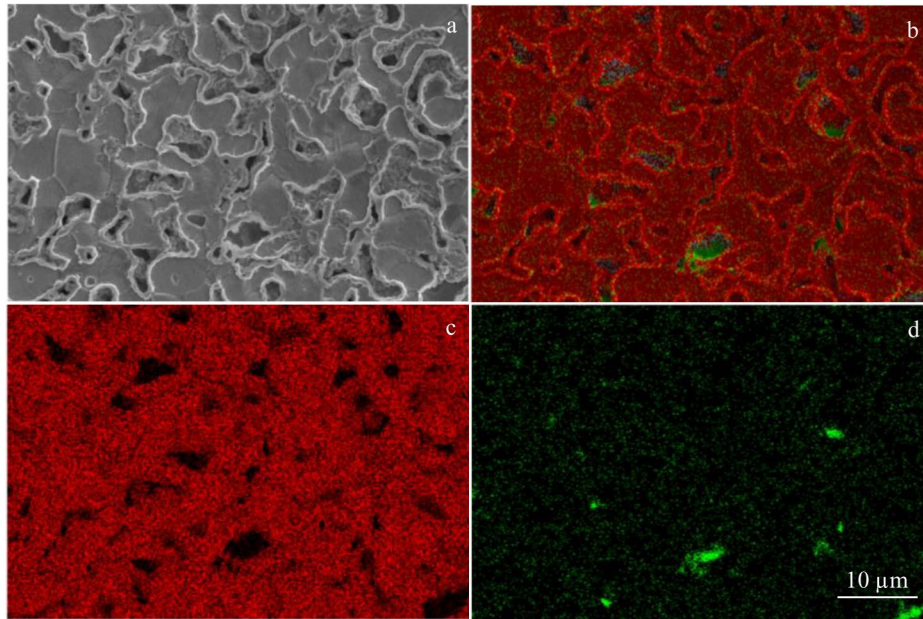


Fig.6 SEM image (a) and EDS layering diagram (b) of Mo-15Cu alloy; element distribution of Mo (d) and Cu (c) in the alloy

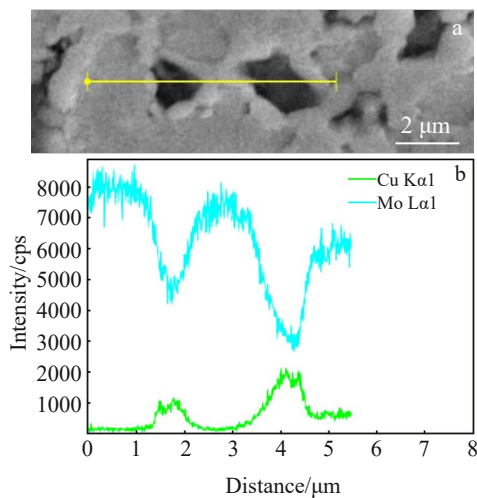


Fig.7 SEM image (a) and EDS line scanning along marked line (b) of Mo-15Cu alloy

phase diffraction pattern is shown in Fig.9c. The diffraction pattern of Mo-Cu is similar to that of the pure Mo diffraction, indicating that Cu atoms are dissolved in Mo crystals, so the Mo-Cu phase is Mo-Cu solid solution. The difference in atomic radii between molybdenum (0.139 nm) and copper (0.1278 nm) is 8.06% and the difference in electronegativity (Mo 2.16, Cu 1.9) is 0.26. According to the theory of Hume-Rothery^[22], if the difference in atomic radii between two substances is less than 15%, they can dissolve into each other and form solid solutions, and according to the theory of electronegativity^[22], if the difference in electronegativity between two metals is less than 0.4, they are more likely to form solid solutions rather than intermetallic compounds. The spiral grinding process in this experiment is a non-equilibrium process. Therefore, the experimental results obtained in this

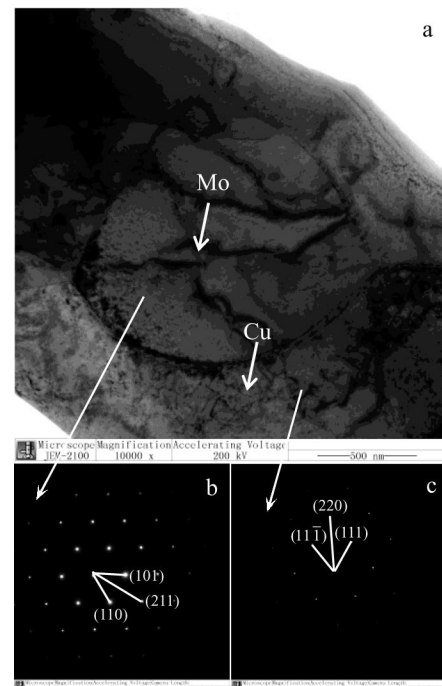


Fig.8 TEM image (a) and SAED patterns of Mo (b) and Cu (c) of Mo-15Cu alloy

study are different from those in equilibrium. The phase relationship between the two phases can be calculated from the coincident spots at the phase boundary of Mo-Cu: $(111)_{Cu} // (110)_{Mo}$ and $[1\bar{1}0]_{Cu} // [1\bar{1}\bar{1}]_{Mo}$.

To further explore the interface characteristics and diffusion mechanism between molybdenum phase and copper phase, the molybdenum-copper interface was analyzed by HRTEM. Fig.10 shows the interface characteristics of Mo/Cu, and the phase interface consists of three region A, B and C. The

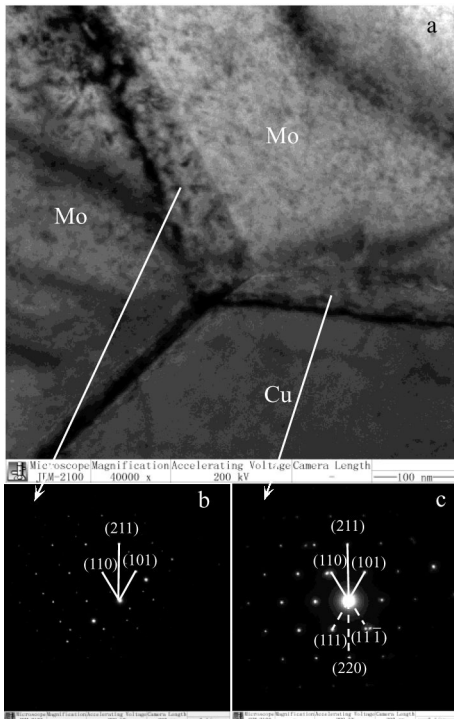


Fig.9 Interface connection characteristics of Mo-Cu interface (a) and electron diffraction recombination spot of Mo/Mo phase (b) and Mo-Cu phase (c)

crystalline surface spacing of the atoms in different alignment directions is 2.061 nm in Fig. 10c. According to the lattice relationship in Fig. 10c, the bottom right area in Fig. 10a is

copper phase, the top left area is molybdenum phase, and the middle layer is Mo-Cu solid solution^[22]. The Mo-Cu solid solution elemental analysis is shown in Fig. 10d. As shown in Fig. 10e, the Mo-Cu solid solution is not detected separately because Mo-Cu solid solution is based on Mo, and its phase structure is similar to that of pure Mo, but the diffraction peak of Mo increases. The lattice arrangement of the copper phase is continuous and regular, while the lattice arrangement of the molybdenum phase is irregular and distributed with a large number of defects (dislocations and vacancies). Since the lattice in region C of the intergranular reaction layer is less mismatched with the lattice of the copper matrix and the atoms are arranged in a similar order, region C contains a higher content of Cu. The order of copper atom content in the reaction layer is region C > region B > region A and the width of the intergranular reaction layer is about 5 nm. The black spherical particle in the Mo phase region in Fig. 10a is the nanotwins formed during the sintering process^[23-24], and Fig. 10b show its enlarged view.

The formation of nanotwins is due to recrystallization in regions with high dislocation density, where the twin boundaries in the nanotwin is related to the dislocation orientation. The formation of nanotwins reduces the degree of mismatch between atoms and releases the internal stress between grains, which reduces the energy of the system. The nanotwins formed at the interface of the molybdenum-copper reaction layer are large in size, and the atomic diffusion in the corresponding copper region is fast, resulting in obvious prominent characteristics of the diffusion layer in the region

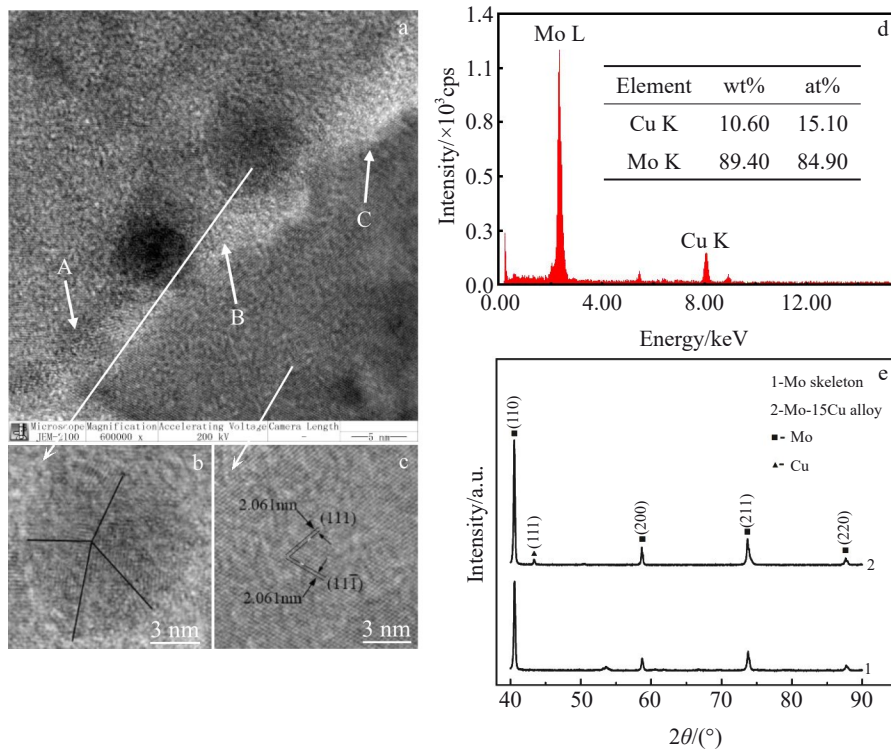


Fig.10 Structural characteristics of Mo-15Cu interface: (a) HRTEM image; (b) nanocrystal partial magnification; (c) copper phase partial enlargement; (d) EDS analysis results of Mo-Cu solution; (e) XRD patterns

C. The region near the nanotwins is a high-density dislocation region, in which defects intensify the diffusion of copper, and promote the formation of intergranular reaction layers. Therefore, the diffusion mechanism of copper element into the molybdenum phase may be vacancy diffusion^[25].

3 Conclusions

1) The submicron-activated layer changes the diffusion mode of Mo-15Cu alloy. The flow and diffusion of Mo particle work together to form the sintered neck and change the growth form of the sintered neck.

2) The nanotwin at the molybdenum-copper interfacial reaction layer accelerates the diffusion of copper atoms and promotes the formation of intergranular reaction layer.

3) The molybdenum phase diffuses into the copper phase and forms an intergranular reaction layer with 5 nm in thickness, which is the main reason for the formation of metallurgical bonding.

References

- Gu Tao, Zhang Shuaixin, Zhao Yuhong et al. *Rare Metal Materials and Engineering*[J], 2021, 50(12): 4224
- Li Y, Wang D Z, Sun A K. *Journal of Central South University*[J], 2013, 20: 587
- Dong L, Ahangarkani M, Chen W G et al. *International Journal of Refractory Metals & Hard Materials*[J], 2018, 75: 30
- Lin D, Han J, Kwon Y et al. *International Journal of Refractory Metals & Hard Materials*[J], 2015, 53: 87
- Zhao Yuchao, Tang Jiancheng, Ye Nan et al. *Rare Metal Materials and Engineering*[J], 2021, 50(4): 1384
- Zhou Hongling, Feng Keqin et al. *Journal of Alloys and Compounds*[J], 2019, 785: 965
- Yao J, Li C, Li Y et al. *Materials and Design*[J], 2015, 88: 774
- Zhou X, Dong Y, Hua X et al. *Materials and Design*[J], 2010, 31(3): 1603
- Kumar A, Jayasankar K, Debata M et al. *Journal of Alloys and Compounds*[J], 2015, 647: 1040
- Chen Q, Liang S, Zhuo L. *Journal of Alloys and Compounds*[J], 2021, 875: 160 026
- Bai Y, Wagner G, Williams C. *Journal of Manufacturing Science & Engineering*[J], 2017, 139(8): 81 019
- Shon J H, Song I B et al. *International Journal of Precision Engineering and Manufacturing*[J], 2014, 15(4): 643
- Chen Q, Liang S, Zhuo L. *Journal of Alloys and Compounds*[J], 2021, 875: 160 026
- Robertson I M, Schaffer G B. *Metallurgical and Materials Transactions A*[J], 2009, 40(8): 1968
- Ke S, Feng K, Zhou H et al. *Journal of Alloys and Compounds*[J], 2019, 775: 784
- Rosalie J M, Guo J, Pippin R et al. *Journal of Materials Science*[J], 2017, 52(3): 9872
- Rajabi J, Muhamad N, Sulong A B et al. *Materials & Design*[J], 2014, 63(21): 223
- Joo Won Oh, Yujin Seong, Seong Jin Park. *Powder Technology*[J], 2019, 352: 42
- Morteza Saghafi Yazdi, Mohammad Talafi Noghani, Najari A. *Journal of Ultrafine Grained and Nanostructured Materials*[J], 2018, 51(2): 153
- Kumar A, Jayasankar K, Debata M et al. *Journal of Alloys and Compounds*[J], 2015, 647: 1040
- Sun C W, Jeong J S, Lee J Y. *Journal of Crystal Growth*[J], 2006, 294(2): 162
- Ke S, Feng K, Zhou H et al. *Journal of Alloys and Compounds*[J], 2019, 775: 784
- Bola Yoon et al. *Ceramics International*[J], 2018, 44(13): 15 176
- Volkman S K, Yin S, Bakhishev T et al. *Chemistry of Materials*[J], 2013, 23(20): 4634
- Du J, Yuan H, Chan X et al. *Journal of Materials Science & Technology*[J], 2018, 34(4): 115

亚微米活化 Mo-15Cu 合金晶间反应机制

王敬泽¹, 尹佳庆¹, 崔建文², 常 晶¹, 于彦东¹, 孙云龙¹

(1. 哈尔滨理工大学 材料科学与工程学院, 哈尔滨 150040)

(2. 哈尔滨工程大学 智能科学与工程学院, 哈尔滨 150006)

摘要: 为了研究具有亚微米组分的钼铜粉末烧结时的晶间反应机制, 采用亚微米活化层法制备了一种具备晶间反应层的钼铜复合材料。采用X射线衍射仪(XRD)、扫描电镜(SEM)、能谱仪(EDS)、透射电镜(TEM)、高分辨透射电镜(HRTEM), 对Mo-15Cu合金组织形貌、连接和结构特征进行了表征。研究了亚微米活化层对钼铜复合材料晶间反应的影响。结果表明, 添加8% (质量分数) 亚微米粉, 可形成厚度约0.5 μm纳米活化层。Mo亚微米颗粒通过流动、扩散, 改变晶间反应机制, 形成了真正意义上的晶间反应层, 厚度约为5 nm, 实现了冶金结合。

关键词: 钼铜伪合金; 纳米孪晶; 晶间反应层; 亚微米活化层; 冶金结合

作者简介: 王敬泽, 男, 1973年生, 博士, 教授, 哈尔滨理工大学材料科学与化学工程学院, 哈尔滨 150040, E-mail: wangjingze310@163.com